

Green's-function quantum Monte Carlo study of a jellium surface

X.-P. Li

*Department of Physics, University of Illinois at Urbana-Champaign, 1110 West Green Street, Urbana, Illinois 61801
and Materials Research Laboratory, University of Illinois at Urbana-Champaign, 104 South Goodwin Avenue, Urbana, Illinois 61801*

R. J. Needs

*Department of Physics, University of Illinois at Urbana-Champaign, 1110 West Green Street, Urbana, Illinois 61801
and Cavendish Laboratory, University of Cambridge, Madingley Road, Cambridge CB3 0HE, United Kingdom*

Richard M. Martin

*Department of Physics, University of Illinois at Urbana-Champaign, 1110 West Green Street, Urbana, Illinois 61801
and Materials Research Laboratory, University of Illinois at Urbana-Champaign, 104 South Goodwin Avenue, Urbana, Illinois 61801*

D. M. Ceperley

*Department of Physics, University of Illinois at Urbana-Champaign, 1110 West Green Street, Urbana, Illinois 61801
and National Center for Supercomputing Applications, University of Illinois at Urbana-Champaign, 405 North Mathews Avenue,
Urbana, Illinois 61801*

(Received 8 July 1991)

A jellium slab at the average valence-charge density of aluminum ($r_s=2.07$) is studied with use of a Green's-function quantum Monte Carlo (GFMC) technique in the fixed-node and diffusion approximations. The trial function is of Slater-Jastrow type, with a pair-correlation term accounting for the anisotropy arising from the surfaces. The GFMC electron density is very similar to that obtained from local-density-approximation (LDA) calculations. The GFMC surface energy is slightly higher than the LDA result and is very close to the value obtained from calculations using the Langreth-Mehl nonlocal-density functional, but significantly lower than predicted by Fermi-hypernetted-chain calculations.

I. INTRODUCTION

Green's-function quantum Monte Carlo (GFMC) methods have been used for calculations on various electronic systems such as light atoms and molecules,¹ the homogeneous electron gas,^{2,3} solid hydrogen,⁴ metal clusters modeled by a jellium background,⁵ and solid silicon.⁶ In this paper we use the GFMC method, in the fixed-node and diffusion approximations, to calculate the surface energy of a jellium slab at the average valence-electron density of aluminum ($r_s=2.07$).

Even within current GFMC algorithms there is room for considerable technical development. Of particular importance are developing better pseudopotentials for real atoms and more accurate trial functions, and removing the fixed-node approximation which is used here to circumvent the fermion sign problem. An important motivation for the present work was to apply the GFMC to a strongly inhomogeneous and anisotropic system to test our current methods for obtaining accurate trial functions. In the study of a jellium surface reported here we have found it necessary to modify the normal form of the Jastrow factor in the trial function to account for the presence of the surfaces.

In the present case we also have the opportunity to test other quantum-mechanical schemes for calculating total energies and surface energies. Because of the simplicity of the model there have been many attempts to calculate the properties of jellium surfaces using different tech-

niques including the local-density approximation (LDA) of density-functional theory,⁷ various nonlocal-density functionals including gradient-correction schemes,⁸ Hartree-Fock theory,⁹ correlated-basis-function methods,¹⁰ and the Fermi-hypernetted-chain (FHNC) approximation.^{11,12} Johnson¹³ performed variational and Green's-function quantum Monte Carlo calculations, but on systems too small and with insufficient accuracy to get a precise value of the surface energy. Numerous LDA calculations for realistic metal surfaces have also been performed which have yielded surface energies in reasonable agreement with experimental values; however, the accuracy of the LDA surface energies of jellium have been questioned. Krotscheck and co-workers have performed FHNC calculations for jellium surfaces for a range of electron densities^{11,12} and have reported large deviations from the LDA results of Lang and Kohn,⁷ which they attributed to the inadequacy of the LDA for strongly inhomogeneous systems. In the conclusion of their paper¹¹ Krotscheck and Kohn state that "the local-density approximation for the particle-hole interactions is inadequate to calculate the surface energy of simple metals." From our GFMC results we will conclude that, at least at the density of $r_s=2.07$ considered here, the FHNC result is inaccurate and the LDA calculations are more reliable. In fact our result is very close to that obtained from density-functional calculations using the nonlocal Langreth-Mehl functions,⁸ which gives some encouragement for such approaches.

The rest of this paper is organized as follows. In Sec. II we describe the GFMC method and give computational details of its application to jellium slabs. In Sec. III we describe the results of our calculations and compare them with other results for jellium surfaces, and in Sec. IV we draw our final conclusions.

II. METHOD AND COMPUTATIONAL DETAILS

A detailed description of the GFMC method in the fixed-node and diffusion approximations can be found in Ref. 1. Let a many-body wave function ψ satisfy the imaginary-time Schrödinger equation

$$\begin{aligned} -\partial\Psi(R,t)/\partial t &= H\Psi(R,t), \\ \Psi(R,0) &= \Psi_T(R), \end{aligned} \quad (1)$$

where H is the Hamiltonian, R represents the electron coordinates, and $\Psi_T(R)$ is an arbitrary trial function. It is simple to show that at large times the wave function $\Psi(R, t \rightarrow \infty)$ approaches the ground-state wave function exponentially fast (to within a normalization constant), as long as the trial function is not orthogonal to the ground state.

In GFMC calculations, Eq. (1) is solved by simulating a diffusion process with branching. We use importance sampling to reduce the statistical error and the fixed-node approximation to circumvent the fermion sign problem. For the trial function we use the standard Slater-Jastrow form

$$\Psi_T(R) = \exp \left[\sum_{i=1}^N \chi(\mathbf{r}_i) - \sum_{1 \leq i < j < N} u(\mathbf{r}_{ij}) \right] D_{\uparrow}(R) D_{\downarrow}(R), \quad (2)$$

where $D_{\uparrow}(R)$ and $D_{\downarrow}(R)$ are Slater determinants of up- and down-spin single-particle states, $u(\mathbf{r})$ is a two-body correlation function, and $\chi(\mathbf{r})$ is a one-body term.

We simulate a surface by using a supercell geometry in

which a unit cell is repeated periodically throughout space. The unit cell that we have used is orthorhombic, being almost square in the xy plane of the surface with dimensions $14.853 \times 14.293 \text{ \AA}^2$, and is 14.004 \AA long in the z direction perpendicular to the surface. This shape was used because it conveniently holds a slab of atomic aluminum, on which we are currently performing similar GFMC calculations. Using the same shape unit cell for the two calculations will facilitate comparison between them. In the present calculations a jellium slab was placed in each unit cell with the normal to the surface in the z direction. The thickness of each slab is equivalent to four layers of aluminum with the surface normal in the $[111]$ direction, which gives a thickness of 9.336 \AA . The slabs are separated from each other by the equivalent of two atomic layers of vacuum (4.668 \AA). Calculations on a variety of thicknesses of aluminum slabs and vacuum regions using the LDA have shown that this geometry is sufficient to give excellent values for the surface energy.¹⁴ This assertion is further supported by the results of the present calculations which will be described later in this paper. The density of the jellium slab is equal to the average valence density of aluminum ($r_s = 2.07$). We applied periodic boundary conditions to the many-body wave function, which then has 360 electron coordinates. The number of electrons (360), determined by the above-described supercell geometry and the average electron density, is large enough to give reliable results. We assumed equal populations of up and down-spin electrons. For this supercell geometry, LDA calculations predict a filled band with an energy gap of 0.05 eV at the Fermi surface. This gap makes it easy to construct the Slater determinants in the trial function, but the *very small* energy gap means the electrons are in delocalized metallic states. With the origin of coordinates at the center of the jellium slab, the potential due to the positive jellium background and the uniform component of the electronic charge is, in atomic units,

$$V(z) = \begin{cases} 2\pi\rho_0[-s(L-s)(L-2s)/3L + (L-2s)z^2]/L, & |z| \leq s \\ 2\pi\rho_0[-s(L-s)(L-2s)/3L + s(-2z^2 + 2|z|L - sL)/L], & s < |z| < L/2, \end{cases} \quad (3)$$

where ρ_0 is the average density within the slab, L is the length of the supercell in the z direction, and s and $-s$ are the positions of the edges of the jellium slab.

The electrostatic energy of the positively charged jellium slabs and the uniform component of the electronic charge density are similar to an Ewald energy because of the periodic boundary conditions in *all* three directions, and are given by

$$E_{\text{Ewald}} = \Omega \frac{2\pi\rho_0^2 s^2}{3L^2} (L-2s)^2, \quad (4)$$

where Ω is the volume of the unit cell.

For the trial function of Eq. (2), the single-particle orbitals in the Slater determinant were generated from an

LDA calculation using a plane-wave basis set including all plane waves up to a cutoff energy of 20 Ry. If we set the Jastrow factor to be 1, that is $u(\mathbf{r})=0$ and $\chi(\mathbf{r})=0$, we recover a wave function whose one-body density is the LDA density. The total energy, E'_{HF} , is slightly higher than the correct Hartree-Fock (HF) energy, but following Ballone,⁵ we use it as a reference to measure the performance of our trial function. This total energy is $E'_{\text{HF}} = 0.8349(52) \text{ eV/electron}$. For a three-dimensional homogeneous electron gas, the two-body term in the Jastrow factor in Fourier space is,³ from the random-phase approximation,

$$u(\mathbf{k}) = \frac{1}{2S_0(\mathbf{k})} + \left[\frac{1}{4S_0(\mathbf{k})^2} + \frac{4\pi}{k^4} \right]^{1/2}. \quad (5)$$

This function is long ranged in real space so it is broken up into a short-range (sr) part and a long-range (lr) part which is expanded in plane waves³

$$\sum_{i < j} u(\mathbf{r}_{ij}) = \sum_{i < j} u_{sr}(\mathbf{r}_{ij}) + \frac{1}{2} \sum_{\mathbf{k}} u_{lr}(\mathbf{k}) \exp(i\mathbf{k} \cdot \mathbf{r}_{ij}). \quad (6)$$

When Eqs. (5) and (6) are used for the two-body term, and the one-body term $\chi(\mathbf{r})$ is adjusted so that the charge density obtained in a variational Monte Carlo (VMC) calculation is close to the LDA density,¹⁵ the VMC energy is very high. Thus we modify Eq. (6) by omitting all the terms with $k_z \neq 0$ in the sum over \mathbf{k} . This is equivalent to using the three-dimensional electron gas form of $u(\mathbf{r})$ in the xy plane, while in the z direction the long-range part is smoothly cut off. The cusp condition for parallel and antiparallel spins is in principle different,³ but because of the Pauli principle, two electrons with parallel spins can rarely be close enough for the cusp condition to become important. Therefore, we use the same cusp condition for both parallel and antiparallel spins (which is correct for antiparallel spins). Test calculations show that this simplification does not affect the energy even in VMC. We then adjust the one-body term $\chi(\mathbf{r})$ repeatedly until the charge density obtained in a VMC calculation with the modified trial function is close to the LDA density. As shown in Figs. 1 and 2, the VMC density is still about 5% different from the LDA density. Our final VMC energy is $E_{\text{VMC}} = -0.0970(35)$ eV/electron, recovering 88% of the correlation energy of the GFMC result. We could have optimized the Jastrow factor more fully than

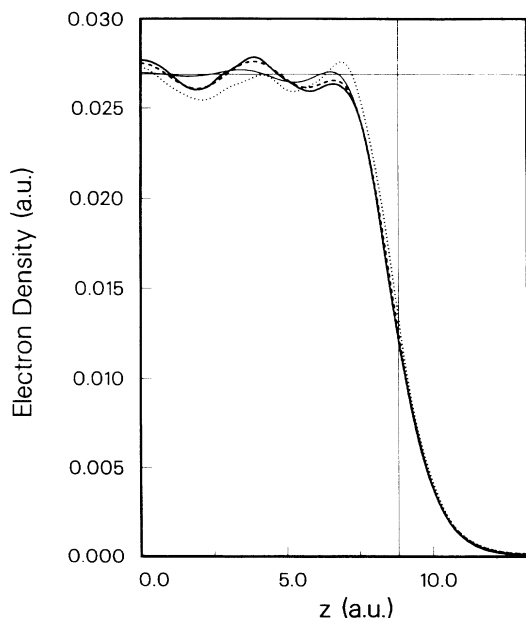


FIG. 1. The electron charge density in the z direction perpendicular to the slab surfaces. The origin is at the center of the slab, the thin vertical straight line at 8.821 a.u. is the jellium edge, and the horizontal thin line is at the average density of the bulk. The thick solid line is the GFMC result, the dotted line is the VMC result, the dashed line is the LDA result with the same periodic boundary conditions applied, and the thin solid line is the full LDA result for this slab geometry.

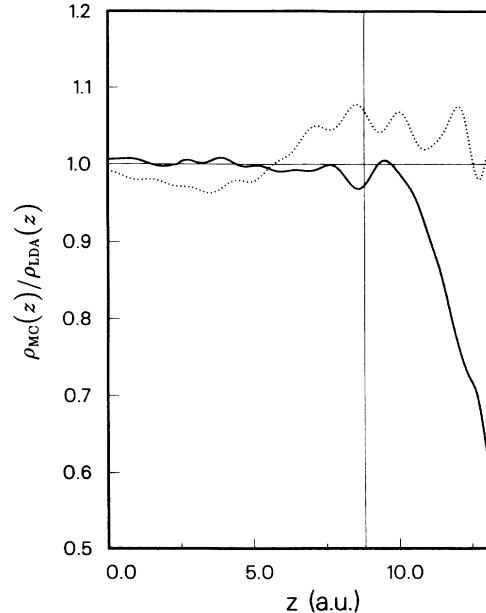


FIG. 2. The ratio of Monte Carlo and LDA charge densities for the finite system. The dotted line is the VMC-LDA density ratio and the solid line is the GFMC-LDA density ratio.

this, using, for example, the Fermi-hypernetted-chain technique developed by Krotscheck, Kohn, and Qian.¹² However, since the GFMC method is very robust with respect to variations of the trial function, we believe that our Jastrow factor is sufficiently accurate.

We used a time step of 0.015 a.u. for the GFMC calculations. Separate tests have shown that the error due to this finite time step is negligible. The total simulation time was 290 simulation blocks, where each block consists of 500 steps of 0.015 a.u. The average population of configurations during the simulation was 200.

III. RESULTS AND COMPARISON WITH OTHER CALCULATIONS

First we describe how we have obtained the GFMC surface energy for jellium which is given in Table I. The

TABLE I. Surface energies of jellium ($r_s = 2.07$).

Method	Surface energy (eV/Å ²)
LDA (Wigner formula) ^a	-0.0456
LDA (Ceperley-Alder formula) ^b	-0.0354
Hartree-Fock ^c	-0.091
Hartree-Fock ^b	-0.141(7)
Langreth-Mehl functional ^d	-0.0302
FHNC ^e	-0.0139
GFMC ^b	-0.029(3)

^aLang and Kohn, Ref. 7.

^bThis work.

^cSahni and Ma, Ref. 9, linearly interpolated between the values at $r_s = 2.0$ and 2.5.

^dZhang, Langreth, and Perdew, Ref. 8.

^eKrotscheck and Kohn, Ref. 11.

energy per electron of the jellium slab from the GFMC calculation is shown in Fig. 3 as a function of imaginary time measured in simulation blocks. After about 100 blocks the system reaches equilibrium. Averaging over the last 200 blocks, we obtain $-0.2294(19)$ eV/electron.

Before calculating the surface energy we must apply a finite size correction to our GFMC jellium slab results, which we obtain from LDA calculations. We have calculated the total energy within the LDA for the same supercell as was used for the GFMC calculations and applying the same periodic boundary conditions to the determinant of single-particle orbitals (i.e., with the same single-particle orbitals as used in our trial function) and for a number of larger supercells in which the thickness of the jellium slab, the thickness of the vacuum region, and the repeat distance within the surface plane were systematically increased. From these results we obtained a finite-size correction which is quite modest, amounting to a correction to the surface energy of -0.0058 eV/Å².

To calculate the surface energy we also require a value for the energy of bulk jellium calculated in the same fixed-node GFMC approximation. Such calculations were performed by Ceperley and Alder¹⁶ who obtained a value of -0.2017 eV/electron. Ceperley and Alder² also performed release-node GFMC calculations for bulk jellium, but it is not currently possible to do such calculations for the jellium slab. However, we expect a large degree of cancellation between the fixed-node error in the slab and the bulk calculations, and therefore we believe that our surface energy is reliable. In fact the release-node correction in bulk jellium is very small at this density, being only -0.0023 eV/electron, but it would be quite inappropriate to apply this correction to the bulk and not to the slab because the energy per electron of the slab would not approach the bulk energy as the thickness

of the slab was increased.

The above analysis gives us a surface energy of $-0.0292(18)$ eV/Å². There are five possible sources for systematic error: (a) the time step error, which we believe is negligible; (b) the finite-size error, which we roughly estimate at 20% of the LDA correction, that is, ~ 0.0012 eV/Å². (c) the fixed-node error (i.e., the difference of the release-node corrections between the slab and the bulk) which should not be more than half of the release-node correction in the bulk, that is, ~ 0.0010 eV/Å²; (d) a possible convergence error of ~ 0.002 eV/Å²; and (e) a possible underestimate of the statistical error (due to sequential correlation) of ~ 0.001 eV/Å². Hence we arrive at our final value for the surface energy of jellium at a density of $r_s = 2.07$ of $-0.029(3)$ eV/Å².

We now compare our GFMC value for the surface energy with the results of other calculations (see Table I). Our value for the LDA surface energy of jellium, using the Ceperley-Alder² exchange-correlation energy as parametrized by Perdew and Zunger,¹⁷ is -0.0354 eV/Å². This is significantly higher than that given by Lang and Kohn⁷ of -0.0456 eV/Å². This difference arises because Lang and Kohn used the Wigner¹⁸ form for the exchange-correlation energy. We have repeated our calculation using the Wigner form, and obtained a surface energy of -0.0436 eV/Å², in close agreement with the result of Lang and Kohn. The GFMC surface energy is therefore a little higher than the LDA value obtained using the Ceperley-Alder form, but the difference is not large. The GFMC surface energy is actually very close to that obtained from density-functional calculations using the Langreth-Mehl nonlocal-density functional⁸ (which is essentially a scheme employing corrections to the LDA involving the gradient of the charge density). The surface energy obtained by Sahni and Ma⁹ is an upper bound to the Hartree-Fock surface energy, and indeed the surface energy from our Hartree-Fock calculation (using the LDA wave functions) is lower than that of Sahni and Ma. However, the Hartree-Fock surface energies from both calculations are much lower than the GFMC surface energy.

The difference between our surface energy and that obtained by Krotscheck and co-workers^{11,12} using the FHNC approximation is large and we can only conclude that the FHNC calculation are inaccurate at this density.

Figure 1 shows the electron density of the jellium slab. The GFMC density (thick solid line) is very close to that obtained from the LDA (dashed line), in agreement with Ballone's results on clusters,⁵ although the input density for the GFMC calculations (VMC density, dotted line) is about 5% off (the GFMC results shown are calculated from the mixed estimate by the linear extrapolation method¹⁹). This provides support for our procedure of constraining the trial function to reproduce the LDA charge density. The LDA density for the slab, but with periodic boundary conditions applied at infinity within the surface plane, is also plotted in Fig. 1 (thin solid line). The oscillations in this charge density (thin solid line) are smaller than in the supercell GFMC and LDA densities. These smaller oscillations are from the combined effects of the finite thickness of the slab and the heavily damped

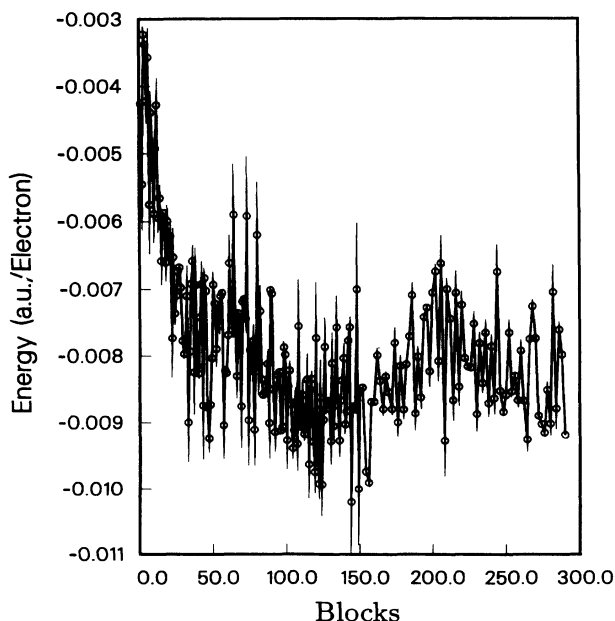


FIG. 3. The GFMC energy of the jellium slab as a function of imaginary time measured in blocks of 500 moves of 0.015 a.u.

Friedel oscillations due to the presence of the surfaces. Note that the charge density in the center of the vacuum region is almost zero, which suggests that the thickness of the vacuum region is adequate. To compare the densities in detail, we plot the ratio of Monte Carlo and LDA densities for the finite system in Fig. 2. The VMC density

is less than the LDA density inside the slab and greater than it outside the slab, reflecting that the Jastrow factor in the trial function is slightly too repulsive. On the other hand, the GFMC density is very close to the LDA density inside the slab, while being much smaller outside. We believe that this result is physical, since the LDA is

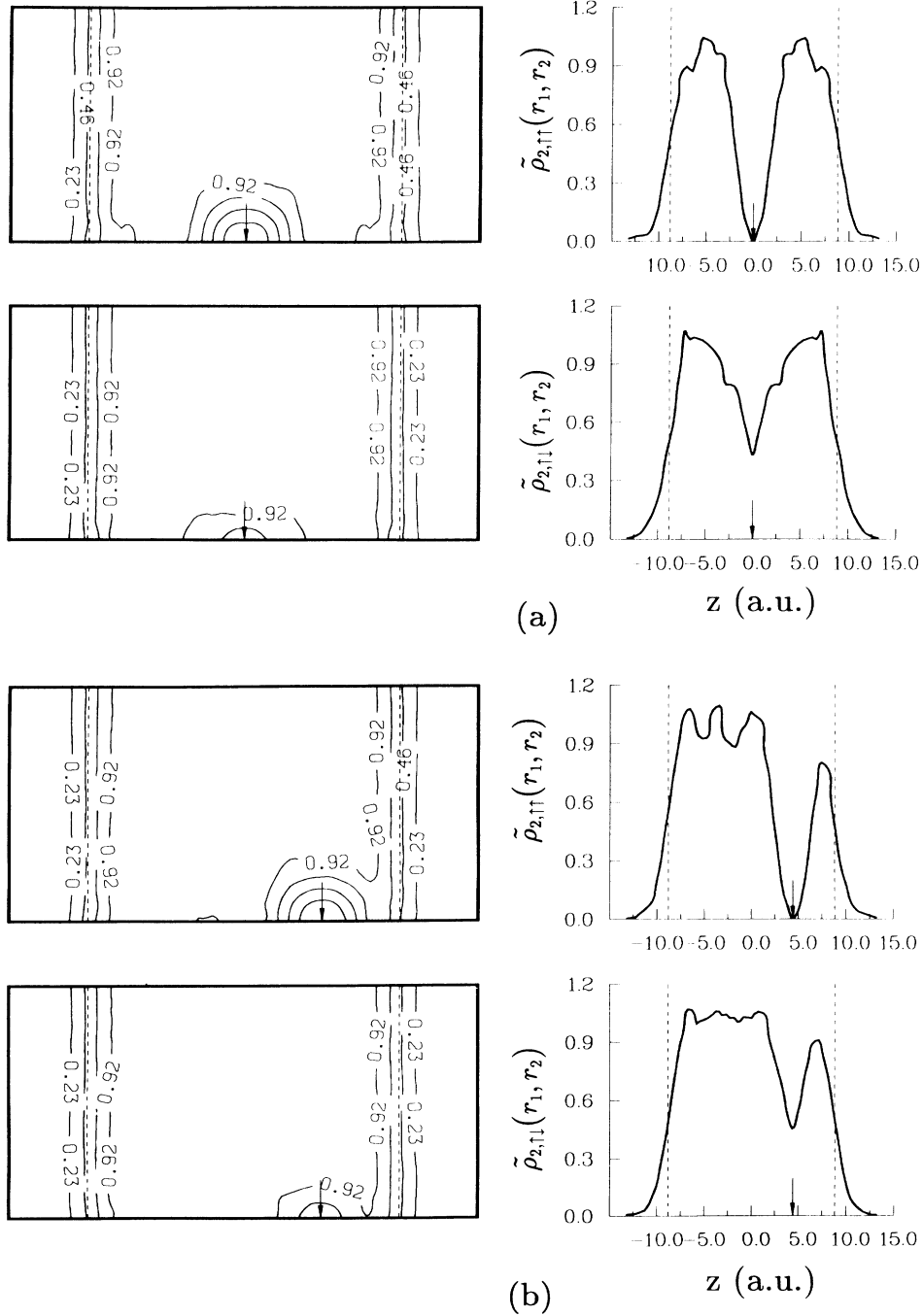


FIG. 4. The normalized pair density $\tilde{\rho}_2(\mathbf{r}_1, \mathbf{r}_2)$ for parallel and antiparallel spins. The upper plots are for parallel spins and the lower ones are for antiparallel spins. The left panels are contour plots, where the horizontal axis is in the z direction (perpendicular to surface), and the vertical axis is in the plane of the surface. In the large area between the contours labeled 0.92, $\tilde{\rho}_2(\mathbf{r}_1, \mathbf{r}_2)$ is close to unity. The right panels show $\tilde{\rho}_2(\mathbf{r}_1, \mathbf{r}_2)$ plotted along the straight line perpendicular to the surface which passes through \mathbf{r}_2 . The dashed lines represent the edges of the positive charge density of the jellium slab, and the arrow indicate the position of \mathbf{r}_1 , (a), (b), (c), and (d) are for different positions of \mathbf{r}_1 .

less accurate when the charge density becomes small and the self-interaction corrections become important.

The normalized pair density $\tilde{\rho}_2(\mathbf{r}_1, \mathbf{r}_2) = \rho_2(\mathbf{r}_1, \mathbf{r}_2) / \rho_0 \rho_1(\mathbf{r}_1)$ measures the correlation between two electrons at \mathbf{r}_1 and \mathbf{r}_2 , where ρ_0 is the average bulk density, $\rho_1(\mathbf{r}_1)$ is the one-body density at \mathbf{r}_1 (plotted in Fig. 1), and $\rho_2(\mathbf{r}_1, \mathbf{r}_2)$ is the pair density defined as the probability of finding one electron at \mathbf{r}_1 and another at \mathbf{r}_2 . Plots of $\tilde{\rho}_2(\mathbf{r}_1, \mathbf{r}_2)$ are shown in Fig. 4 for selected \mathbf{r}_1 points and parallel and antiparallel spins. Some of the oscillatory behavior in these plots is undoubtedly due to statistical noise in the sam-

pling. The normalized pair densities are close to unity when the two electron coordinates are far apart, except near the edge of the jellium slab where they go to zero because the electron density vanishes. There is an exchange-correlation hole when \mathbf{r}_1 and \mathbf{r}_2 are close to each other, and $\tilde{\rho}_{2,\uparrow\uparrow}(\mathbf{r}_1, \mathbf{r}_2)$ goes to zero when $\mathbf{r}_1 = \mathbf{r}_2$ because of the Pauli principle. $\tilde{\rho}_{2,\uparrow\downarrow}(\mathbf{r}_1, \mathbf{r}_2)$ is similar except that the correlation hole is not as deep. When \mathbf{r}_1 is in the center of the slab [Fig. 4(a)] the exchange-correlation holes for parallel and antiparallel spins are, to within the numerical noise, spherical, which indicates that the effect

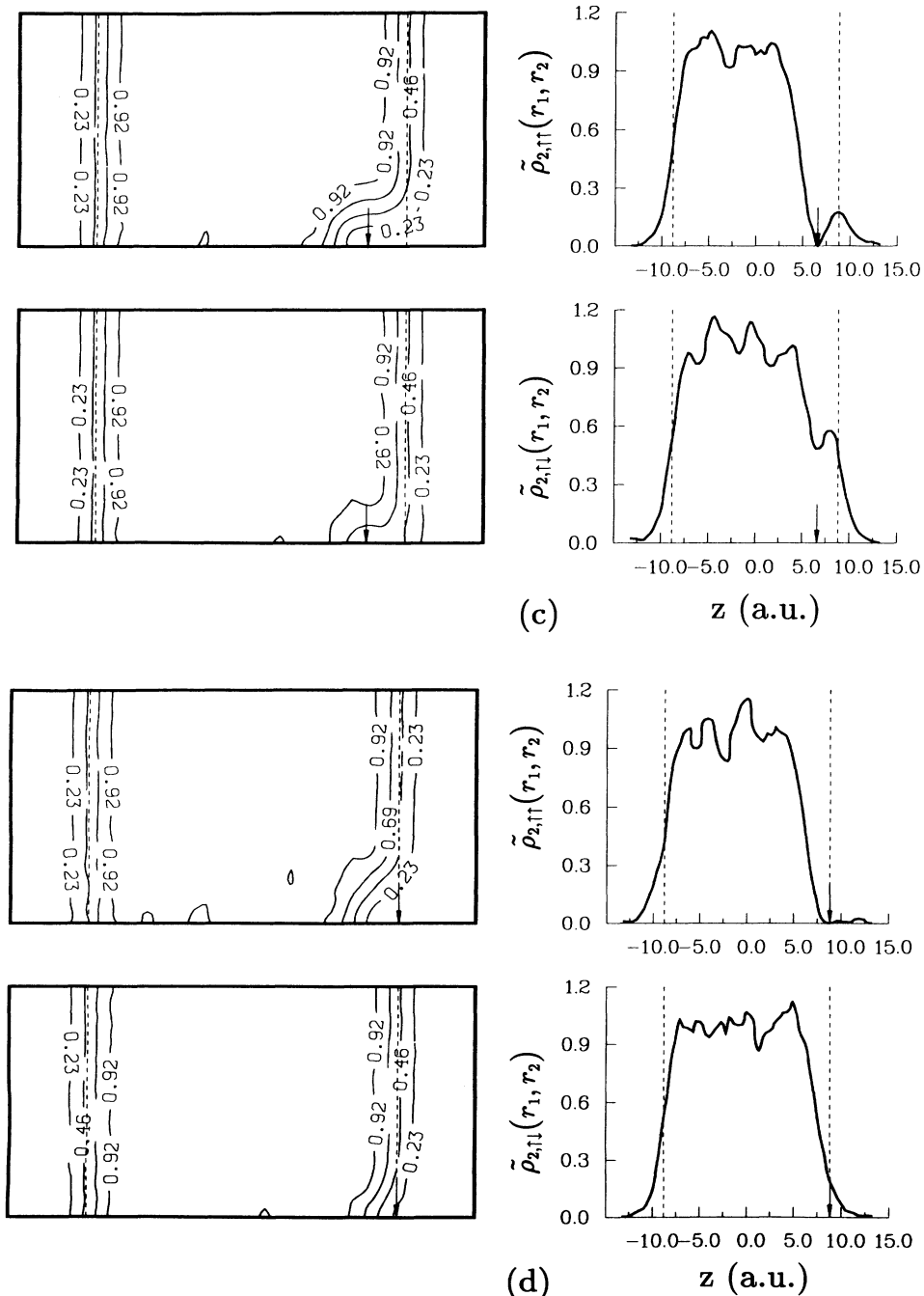


FIG. 4. (Continued).

of the surfaces on electrons near the center of the slab is small. When r_1 is moved toward the edge of the slab the most obvious effect is that the exchange-correlation hole moves with the electron coordinate. When r_1 is close to the surface, the exchange-correlation hole becomes flattened in the plane of surface. It would be interesting to calculate $\bar{\rho}_2(r_1, r_2)$ for r_1 outside of the jellium surface, however this would require development of a special GFMC algorithm. The current code cannot accurately calculate higher-order correlation functions where the electron density is small.

IV. CONCLUSIONS

We have performed a GFMC calculation in the fixed-node and diffusion approximations for a jellium slab at the average valence charge density of aluminum ($r_s = 2.07$). We found that it was necessary to modify the pair-correlation term in the Jastrow factor of the trial function to account for the inhomogeneity and anisotropy arising from the surfaces. We also chose the one-body term in the trial function so as to reproduce, as closely as

possible, the calculated LDA charge density. This appears to be a good procedure in this case because the final GFMC electron density was very close to the LDA result. The GFMC electron density was very close to the LDA result. The GFMC surface energy is slightly higher than the LDA result and is very close to the value from calculations using the Langreth-Mehl nonlocal-density functional. However, our GFMC result is significantly lower than the value obtained from Fermi-hypernetted-chain calculations.

ACKNOWLEDGMENTS

One of us (X.P.L.) would like to thank Dr. G.-X. Qian for helpful discussions. The work of X.P.L., R.J.N., and R.M.M. was supported by the U.S. Department of Energy (Division of Materials Science) under Contract No. DE-AC02-76ER01198, and that of D.M.C. was supported by the National Science Foundation under Grant No. DMR 88-08126. Most of the calculations were performed on the CRAY-YMP at the National Center for Superconducting Applications.

¹P. J. Reynolds, D. M. Ceperley, B. J. Alder, and W. A. Lester, *J. Chem. Phys.* **77**, 5593 (1982).

²D. M. Ceperley and B. J. Alder, *Phys. Rev. Lett.* **45**, 566 (1980).

³D. M. Ceperley, *Phys. Rev. B* **18**, 3126 (1978).

⁴D. M. Ceperley and B. J. Alder, *Phys. Rev. B* **36**, 2092 (1987).

⁵P. Ballone, in *Proceedings of the NATO Workshop in Material Science and Computer Simulations*, edited by M. Meyer and V. Pontikis (Kluwer Academic, Boston, 1991).

⁶X.-P. Li, D. M. Ceperley, and R. M. Martin, *Phys. Rev. B* **44**, 10929 (1991).

⁷N. D. Lang and W. Kohn, *Phys. Rev. B* **1**, 4555 (1970).

⁸Z. Y. Zhang, D. C. Langreth, and J. Perdew, *Phys. Rev. B* **41**, 5674 (1990).

⁹V. Sahni and C. Q. Ma, *Phys. Rev. B* **22**, 5987 (1980).

¹⁰X. Sun, M. Farjam, and C.-W. Woo, *Phys. Rev. B* **28**, 5599 (1983).

¹¹E. Krotscheck and W. Kohn, *Phys. Rev. Lett.* **57**, 862 (1986).

¹²E. Krotscheck, W. Kohn, and G.-X. Qian, *Phys. Rev. B* **32**, 5693 (1985).

¹³L. V. Johnson, Ph.D. thesis, University of California at Berkeley, 1981.

¹⁴R. J. Needs and M. J. Godfrey, *Phys. Rev. B* **42**, 10933 (1990).

¹⁵S. Fahy, X. W. Wang, and S. G. Louie, *Phys. Rev. Lett.* **61**, 1631 (1988); *Phys. Rev. B* **42**, 3503 (1990).

¹⁶D. M. Ceperley and B. J. Alder (unpublished).

¹⁷J. Perdew and A. Zunger, *Phys. Rev. B* **23**, 5048 (1981).

¹⁸E. P. Wigner, *Phys. Rev.* **46**, 1002 (1934); D. Pines, in *Solid State Physics*, edited by F. Seitz and D. Turnbull (Academic, New York, 1955), Vol. 1, p. 367.

¹⁹D. M. Ceperley and M. H. Kalos, in *Monte Carlo Methods in Statistical Physics*, edited by K. Binder (Springer-Verlag, Berlin, 1980).